doi:10.1016/j.jmb.2006.02.038 J. Mol. Biol. (2006) 358, 773–784

JMB

Available online at www.sciencedirect.com

SCIENCE DIRECT®

ELSEVIER

Crystal Structure and Site 1 Binding Energetics of Human Placental Lactogen

Scott T. R. Walsh[1,2] and Anthony A. Kossiakoff[2,3]*

[1]*Department of Molecular and Cellular Biochemistry, Ohio State University, 467 Hamilton Hall, 1645 Neil Avenue Columbus, OH 43210, USA*

[2]*Department of Biochemistry and Molecular Biology University of Chicago, W210 Center for Integrative Science 929 E. 57th Street, Chicago IL 60637, USA*

[3]*Institute for Biophysical Dynamics, University of Chicago, Chicago, IL 60637 USA*

**Corresponding authors*

In primates, placental lactogen (PL) is a pituitary hormone with fundamental roles during pregnancy involving fetal growth, metabolism, and stimulating lactation in the mother. Human placental lactogen (hPL) is highly conserved with human growth hormone (hGH) and both hormones bind to the hPRLR extracellular domain (ECD), the first step in receptor homodimerization, in a Zn^{2+}-dependent manner. A modified surface plasmon resonance method was developed to measure the kinetics for hPL and hGH binding to the hPRLR ECD, with and without Zn^{2+} and showed that hPL has about a tenfold higher affinity for the hPRLR ECD1 than hGH. The crystal structure of the free state of hPL has been determined to 2.0 Å resolution showing the molecule possesses an overall structure similar to other long chain four-helix bundle cytokines. Comparison of the free hPL structure with the 1:1 complex structure of hGH bound to the hPRLR ECD1 suggests that two surface loops undergo conformational changes >10 Å upon binding. An 18 residue Ala-scan was used to characterize the binding energy epitope for the site 1 interface of hPL. Individual alanine substitutions at five positions reduced binding affinity by a $\Delta\Delta G \geq 3$ kcal mol^{-1}. A comparison of the hPL site 1 epitope with that previously determined for hGH indicates contributions of individual residues track reasonably well between hPL and hGH. In particular, residues involved in the zinc-binding site and Lys172 constitute the principal binding determinants for both hormones. However, several residues that are identical between hPL and hGH contribute quite differently to the binding of the hPRLR ECD1. Additionally, the overall magnitudes of the $\Delta\Delta G$ changes observed from the Ala-scan of hPL were markedly larger than those determined in the comparative scan of hGH to the hPRLR ECD1. The structural and biophysical data presented here show that subtle changes in the structural context of an interaction can lead to significantly different effects at the individual residue level.

Keywords: human placental lactogen; X-ray crystallography; human prolactin receptor; surface plasmon resonance; alanine-scanning

Introduction

Placental lactogens (PL) and prolactins (PRL) are pituitary hormones with essential roles in a broad range of biological functions.[1] Human placental lactogen (hPL), also called human chorionic somatomammotropin, is produced only during pregnancy and is involved in stimulating lactation, fetal growth and metabolism. During pregnancy in humans, both hPRL and growth hormone (hGH) are down-regulated. They are replaced by two other hormones: hPL, to induce prolactin-like activities, and a placental growth hormone, an hGH sequence variant that stimulates the GH receptor, but does not cross-react with the PRL receptor.[2]

The biological effects of PRL and GH are triggered *via* a hormone-induced receptor homodimerization

Abbreviations used: ECD, extracellular domain; h, human; hPL, human placental lactogen; hPRL, human prolactin; MAD, multiwavelength anomalous dispersion; MH, mini-helix; o, ovine; p, porcine; PL, placental lactogen; PRL, prolactin; PRLR, prolactin receptor; RIA, radioimmunoassay; SPR, surface plasmon resonance; wt, wild-type.

E-mail address of the corresponding author: koss@bsduchicago.edu

0022-2836/$ - see front matter

process.[3,4] hGH activates both hGHR and hPRLR; however, although it shares 85% protein sequence identity with hGH, hPL does not interact with the hGHR, but activates solely the hPRLR, similar to hPRL (<25% protein sequence identity with hPL and hGH, Figure 1(a)). In order to bind to the hPRLR, both hPL and hGH use a Zn^{2+}-binding site with the hPRLR; whereas, PRL does not.[5,6]

Primate PRL receptor biology functions through extensive cross-reactivity, where biological effects can be induced by PRLs, PLs, and GHs.[1] PLs produced by primates are derived from a GH lineage, while PLs from lower species are derived from a PRL origin.[1,7] The reason for this remains unclear. However, a protein engineering study demonstrated that substitution of the hGH sequence at five positions produced an hPL variant with a site 1 binding affinity similar to that of hGH to the hGHR extracellular domain 1 (ECD1).[6] Thus, hPL represent a unique bridge to study the different molecular recognition properties between the PL and GH receptors signaling pathways.

There is a wide range of literature on cell biological, biophysical, structural, and protein engineering studies for the GH and PRL families;[8–10] however, there have been fewer experimental studies of PLs from human and other species.[6,11–13] In particular, there is no information as to whether the PLs, which are expressed to perform their functions only during very specific situations (i.e. pregnancy), have unique binding characteristics compared to their close biological homologues, PRL and GH.

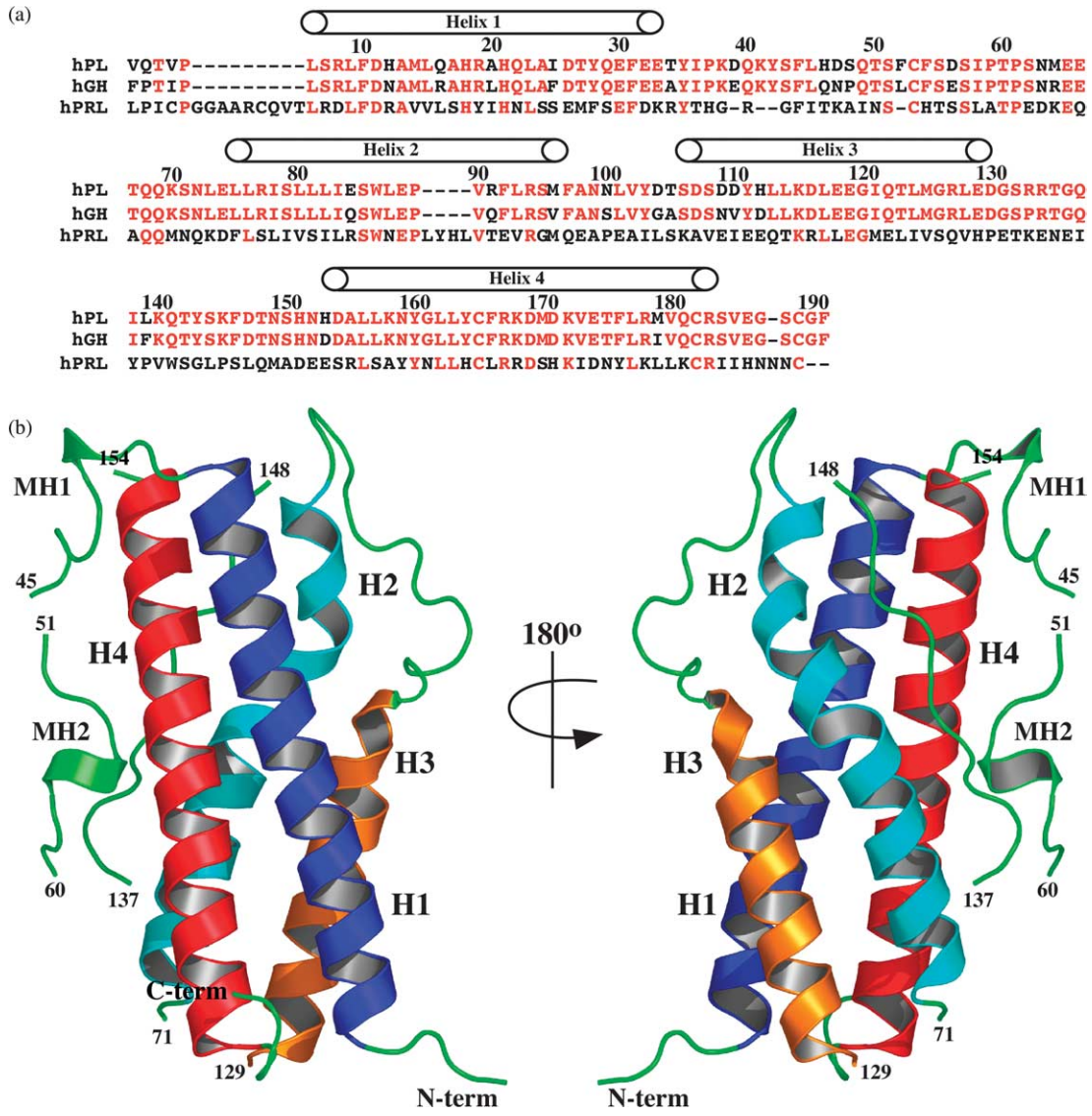

Figure 1. (a) Protein sequence alignments of hPL, hGH, and hPRL determined using default settings in CLUSTAL W.[48] Identical residues are colored red. (b) Ribbon representations of the free hPL crystal structure rotated by 180°. The four α-helices of hPL are numbered and labeled H1–H4, respectively. The two mini-helices are labeled MH1 and MH2. Segments of the polypeptide chain that could not be observed in the electron density maps have been omitted. All structural pictures were generated using Pymol (http://pymol.sourceforge.net/).

In order to further our knowledge of hPL biology from a structural and biophysical point of view, we have determined the crystal structure of the free state of hPL and compared it to hGH from the structure of the 1:1 complex of hGH:hPRLR ECD1.[14] This comparison suggests that two regions of hPL undergo large conformational changes upon binding the hPRLR ECD1. It was known that both hPL and hGH bind the hPRLR ECD in a Zn^{2+}-dependent fashion,[5,6] but the kinetics of the process have not been well characterized. To establish the effects of Zn^{2+} on the binding kinetics of hPL, hPRL, and hGH to the hPRLR ECD1, we have developed a modified surface plasmon resonance (SPR) method that overcomes the inherent non-specific binding effects that were induced by Zn^{2+}. This allowed us to confirm the importance of Zn^{2+} for hPL and hGH binding, and the absence of a direct Zn^{2+} effect in the case of hPRL.

Using an 18 residue Ala-scan, we mapped the site 1 binding energy surface of hPL to the hPRLR ECD1. We found that identical residues in hPL and hGH exhibit different energetic contributions to binding the hPRLR ECD1. The overall magnitudes of the energy differences observed in the Ala-scan of hPL are generally systematically larger than those determined for the same residues in the comparative hGH Ala-scan. There are three residues in hPL that, when mutated to alanine, completely abolish binding; whereas, the same mutations in hGH show significant decreases in binding, but do not eliminate it. Interestingly, the observed effects of the single-site alanine mutations in both hPL and hGH relative to their binding to the hPRLR are generally significantly larger than those seen in the case of wild-type (wt)-hGH to its cognate receptor, hGHR.

Results

hPL structure

The crystal structure of hPL was determined experimentally using multiwavelength anomalous dispersion (MAD) phasing methods.[15] hPL is a 191 amino acid residue protein containing six methionine residues that were converted to seleomethionine to facilitate MAD phasing. The initial maps were calculated using experimental MAD phases to 2.7 Å. The data were extended incrementally and the updated model refined using a native high-resolution data set to 2.0 Å (Table 1). The final

Table 1. Crystallographic data collection and refinement statistics of hPL

Crystal	Native	Peak	Inflection	Remote
A. *Crystallographic data collection*				
Beamline	APS 14-BMD	APS 19-ID		
Wavelength (Å)	1.00	0.97913	0.97929	0.95373
Resolution (Å)	30–1.9	15–2.45	15–2.45	15–2.45
Space group	*C*2	*C*2		
Unit-cell parameters				
a (Å)	115.48	115.63		
b (Å)	30.04	29.97		
c (Å)	53.49	53.51		
$\alpha=\gamma$ (deg.)	90.00	90.00		
β (deg.)	113.38	113.45		
No. reflections				
Observed	47,617	38,430	46,078	23,119
Unique[a]	13,322	6356	6474	6469
Completeness (%)	95.9 (70.6)	99.3 (97.8)	99.4 (97.9)	99.1 (97.9)
Mosaicity	0.28	0.67	0.79	0.81
Average redundancy	3.6 (2.0)	6.0 (6.2)	7.1 (7.3)	3.6 (3.7)
R_{merge}[b]	5.0 (50.3)	15.7 (71.9)	8.9 (37.7)	9.6 (60.7)
Average $I/\sigma(I)$	21.9 (1.5)	17.0 (8.9)	20.1 (6.6)	12.5 (2.3)
Phasing[c]				
Overall figure of merit	SOLVE = 0.48		RESOLVE = 0.71	
B. *Refinement*				
Resolution (Å)	15–2.0			
Protein atoms	1387			
Water molecules	65			
R_{cryst}[d]	0.229			
R_{free}[e]	0.267			
Average *B* values (Å^2)				
Protein atoms	35.9			
Water molecules	41.7			
Stereochemical restraints, rmsd				
Bond lengths (Å)	0.023			
Bond angles (deg.)	2.141			

Values in parentheses are the last data shell of 1.97–1.90 Å and 2.54–2.45 Å for the native and SeMet hPL data, respectively.

[a] For the MAD data set, the Bijvoet pairs were scaled separately.

[b] $R_{merge} = \sum_i |I_i - \langle I \rangle| / \Sigma \langle I_i \rangle$, where I_i is the observed intensity and $\langle I_i \rangle$ is the average intensity over symmetry-equivalent measurements.

[c] Phase information was determined using data from 15–2.7 Å.

[d] $R_{cryst} = \Sigma |F_{obs} - F_{calc}| / \Sigma F_{obs}$, where F_{obs} and F_{calc} are the observed and calculated structure-factor amplitudes.

[e] R_{free} was calculated as for the R_{cryst} factor, using a 10% random subset of all reflections not used during refinement.

model was refined to a crystallographic *R*-factor of 0.229 (R_{free} of 0.267) with 1387 protein atoms and 65 water molecules.

hPL displays the classical long-chain cytokine fold consisting of a four-helix bundle with the α-helices arranged in an up-up-down-down topology with two long cross-over loops similar to that of the structures of hGH, hPRL, and ovine placental lactogen (oPL)[13–17] (Figure 1(b)). The principal four α-helices are comprised of residues 5–36 (helix 1), 72–98 (helix 2), 109–125 (helix 3), and 154–185 (helix 4). There was no interpretable electron density for several loop region residues (61–70, 130–136 and 190–191), indicating a degree of dynamic behavior. Two small α-helices, termed mini-helices (MH), are located at residues 37–41 (MH1) and 53–59 (MH2). There are two disulfide bonds involving residues Cys53–Cys165 and Cys182–Cys189. The Cys53–Cys165 disulfide bond connects loop 1 (50s–60s loop) to helix 4, while the Cys182–Cys189 disulfide bond forms a coil structure at the C terminus of the hPL molecule.

Comparison of hPL to other hormones

The four-helix bundle core of hPL displays a strong similarity to porcine growth hormone (pGH),[18] hGH (3hhr.pdb)[16] and oPL (1f6f.pdb).[13] Figure 2 shows the hPL structure superimposed onto hGH taken from the 1:1 structure of hGH bound to the hPRLR ECD1[14] and oPL bound to the rat PRLR ECDs.[13] (We note that there is no reliable structure of free wt-hGH to compare free hPL with.) The backbone root-mean-square deviation (rmsd) of the backbone atoms between hPL and hGH (from the 1:1 hGH:hPRLR ECD1 complex) for 99 C^{α} atoms of the four-helix bundles is 0.75 Å. Similar backbone rmsd values are obtained for the four-helix bundles for oPL,[13] and other hGH structures bound to the hGHR ECDs.[16,19]

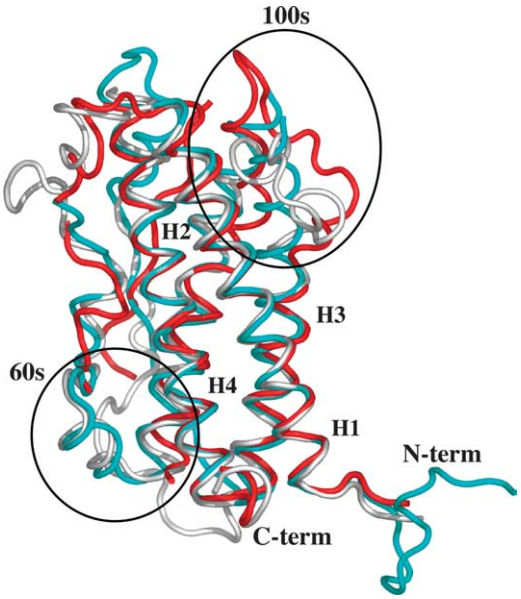

Figure 2. Backbone superimposition of hPL (red tube) onto the structure of hGH (white tube) from the 1:1 complex of hGH bound to the extracellular domain of the prolactin receptor (1bp3.pdb).[14] The structure of ovine placental lactogen (oPL, cyan tube) from the ternary complex of oPL bound to two copies of the rat prolactin receptor ECD is also superimposed onto the hGH structure (1f6f.pdb).[13] The regions that show the most significant changes between the structures are circled and involve residues in the 60s and 100s loop regions. Helices 1 through 4 are labeled accordingly.

The comparison of the free hPL structure to that of the bound form of hGH establishes two regions of significant differences (Figure 2). In the 60s loop region, the residues of hGH adopt a small α-helix that interacts with residues on the hPRLR ECD1. In contrast, there is no clear electron density for this region in free hPL. This dynamic behavior suggests that binding involves some type of disorder to order transition. An NMR relaxation and hydrogen exchange study on the free state of hGH shows no chemical shift assignment in the 60s region due to exchange broadening of the resonances beyond detection and provides further evidence to support this conclusion.[20]

A second region of significant structural difference occurs in the 100s loop region leading into helix 3. The structure in this loop region between the two hormones structurally diverge around residue 85 and returns back into register at residue 110. The greatest distance between identical C^{α} atoms of V102 between hPL and hGH is ~19 Å, with other equivalent atoms on the hormones showing ~8–10 Å displacements. The structural differences seen for this region between hPL and hGH result from hPL displaying a regular loop conformation; whereas, the hGH structure contains a couple of helical turns from L93–N99 and G104–S108. This region has been implicated to be functionally important for binding of the second hPRLR and hGHR ECDs to produce the active ternary 1:2 complex.[16,21,22]

Binding kinetics for the site 1 interaction between hPL and the human growth hormone receptor

A series of multiple mutations (based on previous work by Lowman and Wells) were introduced into hPL, which increased site 1 binding to the hGHR ECD1 by ~300-fold.[6] The study described here was undertaken to normalize the data obtained for the hPL-hPRLR binding with the previously determined hGH-hPRLR binding data that were obtained by radioimmunoassay (RIA) analysis.[23] The site 1 binding kinetics of wt-hPL to the hGHR ECD1 displays a k_{on} rate constant of $1.5\times10^{5}\,M^{-1}\,s^{-1}$ and a k_{off} rate constant of $1450\times10^{-4}\,s^{-1}$ (Table 2). The resulting K_d of 967 nM is similar to the value of 770 nM determined by RIA (Table 2).[6] The large difference in K_d for hPL (K_d = ~1 μM) compared with hGH (K_d = 1.2 nM) binding to the hGHR ECD1 is almost exclusively due to a ~370-fold faster k_{off} rate constant for wt-hPL.

Table 2. SPR binding kinetics of hPL variants to the hGHR ECD1

Hormone variant	k_{on} (M^{-1} s^{-1})$\times 10^5$	k_{off} (s^{-1})$\times 10^{-4}$	K_d[a] (nM)	K_d (wt) K_d(vari)	RIA[b] (nM)
hGH[c]	3.2	3.9	1.2	1	0.34
hPL	1.5	1450	967	1	770
V4I,D56E,M64K-hPL	0.61	6.4	10.5	92	nd[d]
V4I,D56E,M64K,M179I-hPL	1.0	7.0	7.0	138	3.8
V4I,D56E,M64K,M179I,E174A-hPL	1.2	3.9	3.3	293	0.56

Experiments were performed in 10 mM Hepes (pH 7.4), 150 mM NaCl, 3 mM EDTA, 0.005% (v/v) TWEEN-20 at 25 °C.
[a] Equilibrium dissociation constant: $K_d = k_{off}/k_{on}$.
[b] Reported K_d values determined by radioimmunoassay experiments given by Lowman *et al.*[6]
[c] Reported SPR binding kinetics taken from Bernat *et al.*[27]
[d] Not determined.

Incorporating three mutations based on the hGH sequence (V4I, D56E, and M64K) increased its binding affinity to hGHR ECD1 by almost 90-fold ($K_d = 10.5$ nM) (Table 2). The effect of the V4I mutation is somewhat surprising, because it was shown in the case of hGH to be less important for site 1 binding and more critical for second hGHR ECD2 binding.[22] Introducing M179I and E174A into the triple-mutant background further increased the binding affinity by an additional 3.3-fold ($K_d = 3.3$ nM). This hPL pentavariant is only 2.8-fold weaker than wt-hGH binding to the hGHR ECD1. The higher binding affinities of these hPL variants result from a systematic decrease of the k_{off} rates with relatively constant k_{on} rates. Although the absolute K_d values of the hPL pentavariant were found to differ between the SPR and RIA methods by about sixfold, the ratio of the K_d values for wt-hGH *versus* the hPL pentavariant are virtually the same in both (2.8 *versus* 1.6).

Although the hPL pentavariant has a wild-type-like affinity (similar to wt-hGH) for site 1 binding, it was an open question as to whether this variant could bind a second hGHR ECD to form a stable ternary complex. The site 2 interface of wt-hGH has been shown to be highly adaptable to alanine mutations, with no highly defined binding hot-spot.[22] The largest changes seen in second hGHR ECD2 binding were 23-fold (I4A-hGH), 13-fold (R16A-hGH), and 19-fold (N109A-hGH) decreases.[22] Analytical size-exclusion chromatography was used to determine whether the hPL pentavariant could dimerize two copies of the hGHR ECD. Over-titration of this variant with excess hGHR ECD resulted in two distinct peaks, one corresponding to the 1:1 complex of the hPL pentavariant with hGHR ECD and the other corresponding to free hGHR ECD (data not shown). The binding affinity for a second hGHR ECD to the 1:1 pentavariant-hPL hGHR ECD1 complex was determined using an SPR-based steady-state binding affinity model where the maximal SPR response (R_{max}) was plotted against the concentration of the hGHR ECD2 and fitting the binding curve using Scatchard analysis. The second hGHR ECD2 display an apparent K_d of 647 nM to the 1:1 pentavariant-hPL: hGHR ECD1 complex. This is ~170-fold weaker than the wild-type site 2 binding of hGH with hGHR ECD2 (K_d of 3.8 nM).[22] This indicates that the hPL pentavariant does not dimerize the hGHR ECDs to a substantial degree and suggests that there are several non-identical residues in site 2 of hPL that have to be mutated to their hGH equivalent to convert it into a functional hormone for hGHR signaling (candidates for modification are H12N and Q16R going from an hPL to an hGH residue; Figure 1(a)).

Site 1 binding kinetics of hPL, hGH, and hPRL to hPRLR ECD1

To determine the binding kinetics for wt-hPL and various hPL variants to the hPRLR ECD1, a new SPR methodology was developed to eliminate the large non-specific binding effects due to the presence of Zn^{2+} (see Materials and Methods). Both hPL and hGH require Zn^{2+} for binding to the hPRLR ECD1, whereas hPRL does not.[5,6] On the basis of this difference, the binding of hPRL to hPRLR ECD1, in either Zn^{2+} or EDTA buffer, which was used as a control to ensure that all non-specific binding effects due to using Zn^{2+} buffer were eliminated. The site 1 binding affinity of hPRL to the hPRLR ECD1 in the presence of 50 μM $ZnCl_2$ was determined to be 4.2 nM (Table 3). Similar binding kinetics were observed in 3 mM EDTA ($K_d = 5.7$ nM). The K_d values for both hPRL measurements agree well with those determined previously using competition RIA.[6] A recent SPR hPRL:hPRLR ECD study, immobilizing G129C-hPRL to the sensor chip and flowing hPRLR ECD1 over the surface reports an approximately sixfold weaker site 1 binding affinity of 60.5 nM than the value reported here.[24]

As expected due to the Zn^{2+} dependence, the site 1 binding kinetics of hGH and hPL in EDTA buffer showed a marked decrease in overall binding affinity to the hPRLR ECD1 compared to hPRL (Table 3). In EDTA buffer, hGH has a K_d of 349 nM, which agrees well with previously determined RIA measurement of 270 nM.[6] No binding was observed for hPL to the hPRLR ECD1 in EDTA buffer. In Zn^{2+} buffer, hPL and hGH have similar on-rates of 3.7×10^4 and 2.7×10^4 M^{-1} s^{-1}, respectively (Figure 3). However, hPL dissociates from the hPRLR ECD1 an order of magnitude more slowly than does hGH,

Table 3. SPR binding kinetics of the hormones to the hPRLR ECD

	3 mM EDTA				50 μM $ZnCl_2$			
Hormone	k_{on} (M^{-1} s^{-1})×10^5	k_{off} (s^{-1})×10^{-4}	K_d[a] (nM)	RIA[b] (nM)	k_{on} (M^{-1} s^{-1})×10^4	k_{off} (s^{-1})×10^{-4}	K_d (nM)	RIA[b] (nM)
hPRL	1.7	7.1	4.2	2.8	8.4	4.8	5.7	2.6
hGH	0.43	150	349	270	2.7	1.5	5.6	0.033
hPL	nd	nd	NB[c]	NB	3.7	0.22	0.6	0.046

Experiments were performed for the EDTA buffer in 10 mM Hepes (pH 7.4), 150 mM NaCl, 3 mM EDTA, 0.005% (v/v) TWEEN-20. Experiments in Zn^{2+} buffer contained 10 mM Tris–HCl (pH 7.4), 150 mM NaCl, 50 mM $ZnCl_2$, and 0.05% TWEEN-20.
[a] Equilibrium dissociation constant: $K_d = k_{off}/k_{on}$.
[b] Reported K_d values determined by radioimmunoassay experiments given by Lowman *et al.*[6]
[c] No detectable binding.

$k_{off} = 0.22\times10^{-4}\ s^{-1}$ *versus* $1.5\times10^{-4}\ s^{-1}$. The site 1 K_d value for hGH binding to hPRLR ECD1 is 5.6 nM compared to 0.6 nM for hPL. We note that both these values are significantly higher than those obtained by RIA analysis,[6] but it has been observed that SPR and RIA measurements in this system show this systematic trend.[22,25]

Site 1 hPL Ala-scan to the hPRLR ECD1

Using the 1:1 crystal structure of hGH bound to the hPRLR ECD1[14] combined with the previously determined site 1 Ala-scan of hGH to hPRLR ECD1,[23] an 18 residue Ala-scan of hPL was designed that encompassed residues in helices 1, 4, and the 50–60s loop regions. There are only two residue changes between hPL and hGH in the site 1 binding interface: M64 (R64 in hGH) and I25 (F25 in hGH). The hPL site 1 Ala-scan binding results along with the corresponding hGH Ala-scan are given in Table 4.

Virtually all alanine variants of hPL display similar k_{on} rates that are close to the average value of $4.7\times10^4\ M^{-1}\ s^{-1}$ and the wt-hPL k_{on} rate of $3.7\times10^4\ M^{-1}\ s^{-1}$. The binding affinity changes produced by the individual alanine substitutions in hPL are once again shown to be principally off-rate driven (Table 4). Alanine substitutions at 12 of the 18 residues result in decreases in binding affinity of $\Delta\Delta G$ values $\geq$2.0 kcal mol^{-1}. Alanine substitutions of two Zn^{2+} ligands (H18 and E174) and K172 completely abolish hPRLR ECD1 binding (translates into a $\Delta\Delta G$ difference of $>$4.4 kcal mol^{-1} at 25 °C).

Overall, the absolute magnitudes of the $\Delta\Delta G$ changes for the alanine substitutions in hPL are generally larger than for its hGH counterpart; however, the relative values of the 18 site 1 alanine mutations track reasonably well, with several notable exceptions (Table 4). The three hPL residues mentioned above that effectively eliminate binding to the hPRLR ECD1, also show similarly large $\Delta\Delta G$ changes with hGH. However, there are several others that differ significantly between the two hormones. Three of these outlying residues, N63A, M64A and E65A, are in the 60s loop, and two others, Y164A and D171A, are located on helix 4.

Discussion

Comparison of the site 1 binding hot-spot regions in hPL and hGH

As noted above, virtually all the changes in affinities for the hPL variants binding to either the hGHR or the hPRLR ECDs are due to differences in off-rates. This property suggests that the binding transition state energy is not affected significantly by factors at the level of the structural changes introduced by the mutations, even among variants that result in large decreases in binding affinity. A similar trend in binding kinetics has been seen for site 1 and site 2 binding variants of hGH and hGHR ECD1 and ECD2,[19,22,25–29] interleukins-2[30] and

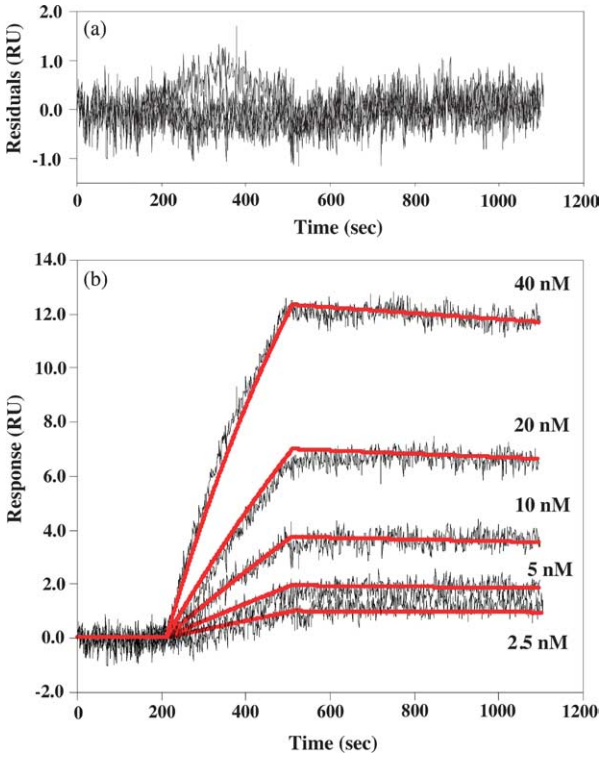

Figure 3. Site 1 binding kinetics of wt-hPL interacting with the immobilized hPRLR ECD1 measured by surface plasmon resonance at 25 °C. The residuals are plotted above the binding sensorgrams.

Table 4. hPL and hGH site 1 Ala-scans to the hPRLR ECD1

Mutant	k_{on} ($M^{-1}s^{-1}$)$\times 10^4$	k_{off} (s^{-1})$\times 10^{-4}$	K_d[a] (nM)	K_d(Ala)/K_d(wt)	$\Delta\Delta G$(hPL)[b] (kcal mol^{-1})	$\Delta\Delta G$(hGH)[c] (kcal mol^{-1})
H18A	nd	nd	NB[d]	NB	>4.4	2.9
H21A	6.7	11.6	17	28	2.0	2.7
I(F)[e]25A	8.5	7.8	9.2	15	1.6	1.2
S51A	3.4	2.0	5.9	10	1.4	nd
I58A	4.4	8.7	20	33	2.1	1.7
S62A	4.9	8.8	18	30	2.0	1.4
N63A	3.2	10.4	33	55	2.4	0.87
M(R)64A	7.5	6.0	8.0	13	1.5	0.35
E65A	5.3	4.5	8.5	14	1.6	0.54
Y164A	6.8	11.3	17	28	2.0	0.44
R167A	2.0	17.9	90	150	3.0	3.9
K168A	1.8	12.1	67	112	2.8	1.7
D171A	7.2	11.0	15	25	1.9	0.057
K172A	nd	nd	NB	NB	>4.4	3.2
E174A	nd	nd	NB	NB	>4.4	3.5
T175A(S)[e]	4.2	12.2	29	48	2.3	0.49
F176A	1.9	19.0	100	167	3.0	1.9
R178A	3.2	12.3	38	63	2.5	1.2

Experiments for hPL were conducted in 10 mM Tris–HCl (pH 7.4), 150 mM NaCl, 50 μM $ZnCl_2$, 0.05% (v/v) TWEEN-20 sat 25 °C. T175S-hGH was reported.[23]

[a] Equilibrium dissociation constant: $K_d = k_{off}/k_{on}$.

[b] $\Delta\Delta G = RT \ln K_d$ (Ala)/K_d (wt)

[c] $\Delta\Delta G$ values determined by radioimmunoassay experiments given by Cunningham &Wells.[23]

[d] No detectable binding.

[e] hGH residue in parentheses.

-4,[31,32] erythropoietin,[33] and granulocyte colony-stimulating factor (G-CSF).[34]

The $\Delta\Delta G$ changes determined for the site 1 Ala-scan of hPL are mapped onto the surface of the molecule in Figure 4(a). The pattern of the energy distribution in the interface indicates that there is a very extensive binding hot-spot region on the hPL surface that involves six residues with $\Delta\Delta G$ decreases $\geq$2.5 kcal mol^{-1}: one in helix 1 and five in helix 4. Substitutions at six additional residues produced $\Delta\Delta G$ effects $\geq$2.0 kcal mol^{-1}. These residues together form an expanded region that encompasses 12 residues, most of which extend from the rigid scaffolds of helix 1 and helix 4. However, three are located on the 60s loop, which appears highly dynamic before binding.

The site1 Ala-scan of hGH (Figure 4(b)) to the hPRLR ECD1 is qualitatively similar to that determined here for hPL.[23] However, the observed effects are generally smaller overall for hGH than for hPL. We note that complementary Ala-scan of the hPRLR site 1 residues additionally indicates that the corresponding $\Delta\Delta G$ changes found for binding to hPL are also larger than those for hGH (our unpublished results). Thus, we feel that the overall magnitude differences are real, but it is hard to quantify the disparity exactly because of the differences in the methods used to collect the two data sets. We note one potential difference in the previously determined RIA measurements was that the hGH alanine mutants were only purified to a level of 60%.[23] Here, the hPL alanine mutants were greater than 95% pure.

Nevertheless, there are several notable differences that cannot be due to scaling effects between the two methods. For example, H21A exhibits a larger binding free energy change for hGH than hPL (2.7 *versus* 2.0 kcal mol^{-1}), which is opposite to the general trend. Y164A and K168A in hGH contribute disproportionally less to binding compared to their function in the hPL interaction with the receptor ECD (Table 4). However, the largest differences between the two Ala-scans are in the six residues in the 50s–60s loop. Ala substitutions in hGH display small decreases in binding in contrast to the very large ones observed for hPL. This extended loop in free hPL (and presumably hGH) is highly dynamic, but becomes ordered on binding. It has been shown that distal mutations of the type that are characteristic of the sequence differences between hPL and hGH can produce significant effects in the population distribution of loop conformations that are 20 Å from the mutation in hGH.[28] Thus, the disparity in the binding energy effects of the 50s–60s loop seen between the two hormones may be due to the difference in energy required to order the loop during binding for the two hormones.

Structural correlation with the site 1 Ala-scans of hPL and hGH

Since the crystallization of the 1:1 hPL:hPRLR ECD1 complex has so far been unsuccessful, there is no direct structural information about the details of the interactions at the hPL-hPRLR ECD1 Site1 interface. However, we feel comparison of the structures of free hPL with that of the bound hGH:hPRLR ECD1 provides a reasonably good model for the nature of the structural transition that occurs between the free and bound states of hPL. Superimposing hPL onto hGH in the 1:1 hGH:hPRLR ECD1 complex reveals that the

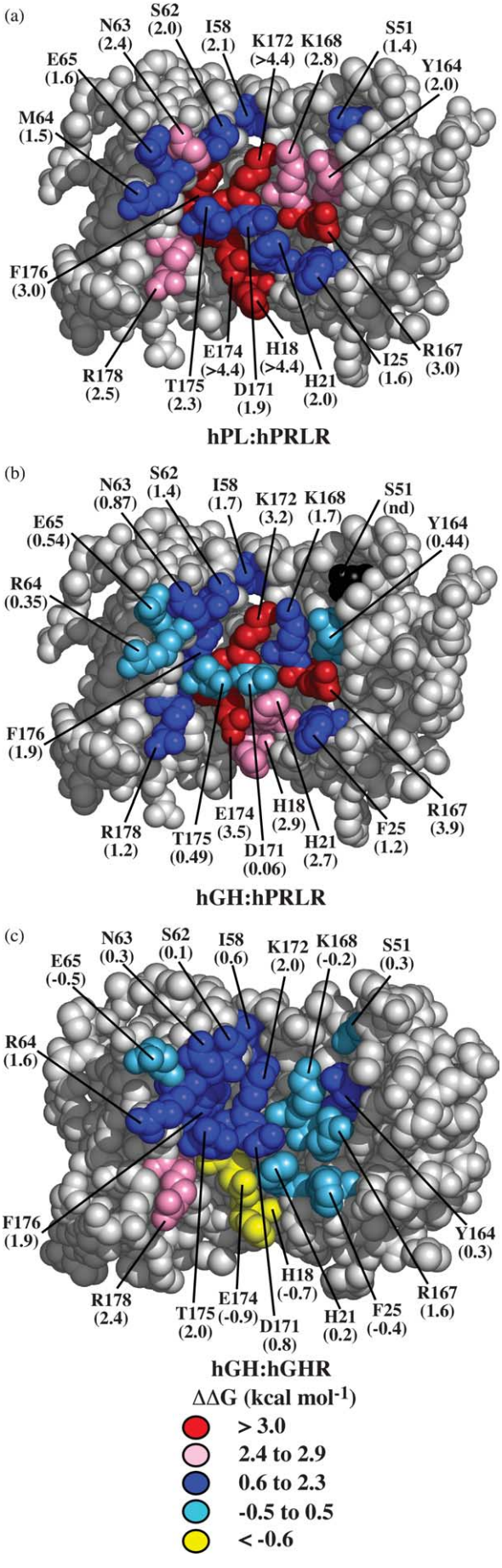

mainchain of the principal hot-spot residues in helix 1 and 4 of hPL requires little or no changes to form specific interactions with hPRLR ECD1 (Figure 5). This suggests that few significant entropic barriers exist for residues on the helices on binding. For instance, the sidechain of Arg178 in free hPL would need to undergo a rotameric shift to position its $N^{\eta 1}$ and $N^{\eta 2}$ atoms to form multiple salt brides to the F140 O, T141 $O^{\gamma 1}$, and Q163 $O^{\varepsilon 2}$ atoms of the hPRLR ECD1 (Figure 5(a)).[14] Likewise, the side-chains of the hot-spot residues of Y164, R167, K172, and F176 of hPL can adopt their bound conformations with small rotational motions and displacement of several bound waters molecules (Figure 5(b) and (c)). These movements would require energies $<kt$ and thus, would be sampled with little or no entropic barrier.

A principal determinant for binding of both hPL and hGH to the hPRLR ECD1 involves a Zn^{2+}-binding site mediated by four ligands, two on the hormone (H18 and E174) and two on the receptor (D187 and H188) (Figure 5(d)). In the hPL crystal structure the carboxylate oxygens of E174 form hydrogen bonds to the $N^{\delta 1}$ atoms of both H18 and H21, essentially preorganizing the hormones' Zn^{2+} ligands prior to binding. A similar preorganization of hydrogen bonding pattern for the sidechain of E174 was observed in the 1:1 hGH:hGHR ECD1 structure.[19]

While the above mentioned hot-spot residues appear to be in "poised" positions to form productive interactions with receptor groups on binding, this is not the case for the hot-spot residues in the 50s–60s loop. The nature of the disorder-to-order transition required for binding cannot be determined in detail; however, it would be supposed some entropic barriers have to be overcome during the binding event. Based on observations from other similar complexes, it is likely that the nature of the disorder in the loop in the free hormone is due to it adopting a few low energy conformations that can interconvert

Figure 4. Site 1 Ala-scans of the hPL and hGH to their receptors. The results are color-coded as a function of $\Delta\Delta G$ (kcal mol^{-1}) at 25 °C. (a) CPK representation showing the site 1 Ala-scan of hPL to the hPRLR ECD1 determined by surface plasmon resonance. The hGH:hPRLR ECD1 crystal structure was used for the Figure. (1bp3.pdb)[14] due to the lack of electron density for the 60s region of residues in the free hPL crystal structure. (b) CPK diagram of the site 1 Ala-scan of hGH to hPRLR ECD1 determined by competition radioimmunoassay.[23] The hGH:hPRLR ECD1 crystal structure was used for this Figure. Ser51 to alanine of hGH was not determined for hPRLR ECD1 binding and is colored black. (c) Surface representation of the site 1 Ala-scan of hGH to the hGHR ECD1 determined by surface plasmon resonance.[23] The 1:1 complex of the hGH:hGHR ECD1 crystal structure was used to generate the representation (1a22.pdb).[19] The $\Delta\Delta G$ values are listed in parentheses for the alanine mutations on the hormones.

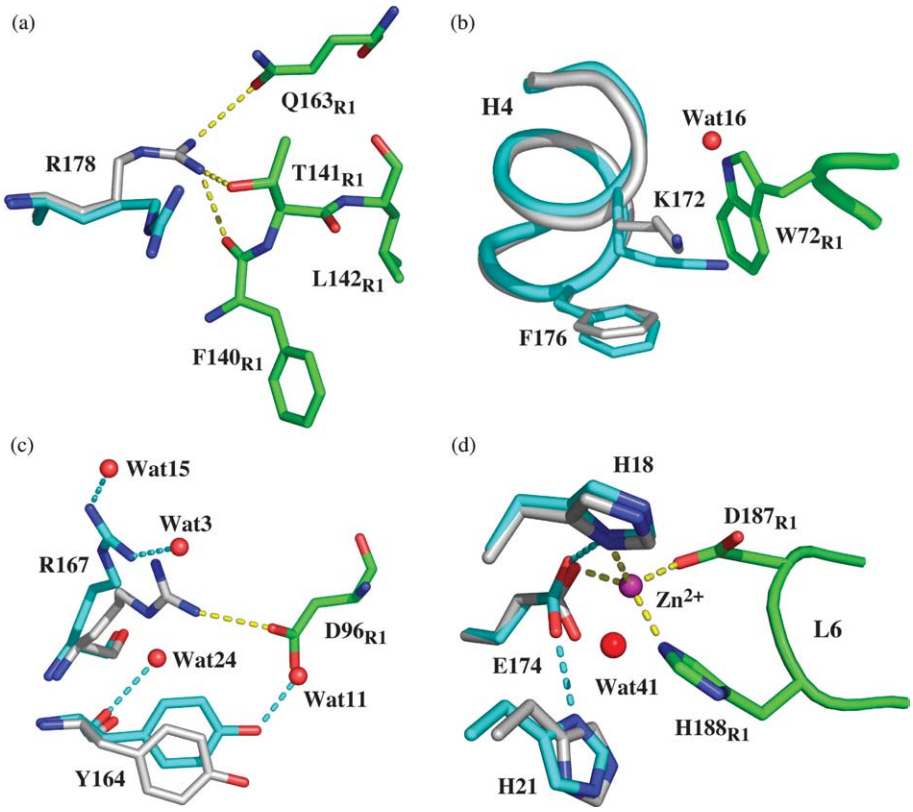

Figure 5. Detailed structural comparison of free hPL compared with the 1:1 complex of hGH:hPRLR ECD1 of the regions where significant binding energy changes occurred determined from the Ala-scan data. hPL residues are colored cyan, hGH and hPRLR ECD1 residues are colored white and green, respectively. Hydrogen bonds in the hPL structure are depicted as broken cyan lines. Water (Wat) molecules are taken from the hPL structure. The intermolecular hydrogen bonds are shown as broken yellow lines between hGH and hPRLR ECD1. (a) Diagram showing the region around Arg178 of the hormones. (c) Diagram around Y164 and R167 of the hormones. (b) Depiction of the hormone residues around K172 and F176. (d) Representation of the Zn^{2+}-binding site for hPL and hGH. The zinc ion is represented as a magenta sphere.

through a relatively few number of peptide rotations.[28]

Differences in the binding interface

Perhaps the most intriguing aspect of the analyses of the energetic landscapes of these hormones and receptors is how different they are, even though in most cases the physical interactions themselves are probably very similar. This is evident by comparing the differences seen between hGH's binding to hGHR ECD1 versus hPRLR ECD1. The structural epitopes are virtually identical, but the functional epitopes, as defined by the size and location of the binding hot-spots are quite different. The binding of hGH to the hPRLR ECD1 involves a larger set of functionally important residues than it does to its cognate receptor, hGHR ECD1 (Figure 4(b) and (c)). Moreover, the functional epitope determined for hPL is significantly larger than compared for the hGH:hPRLR ECD1 interaction. This difference may be in part due to the dual functional role of hGH, which is required to bind and activate two receptors: hGHR and hPRLR. There are specific residues, in particular the Zn^{2+} binding ligands needed for hPRLR binding that are actually inhibitory to hGHR binding. hPL has evolved from an earlier primate GH to bind specifically to hPRLR so that there was no pressure to co-evolve the hormone to two distinct receptor targets and thus it is able to bind the hPRLR ECD2 with higher affinity than hGH.

The Ala-scan data suggest that the Site 1 hPRLR ECD1 binding energy landscape is more extensive than its hGHR counterpart, since more hormone residues contribute to the binding hot-spot and the Zn^{2+} binding ligands are essential for productive binding. It has been shown that the Site 1 residues of hGH act in a very additive fashion when binding to hGHR ECD1.[26] Interestingly, the complementary hGH receptor ECD Site 1 residues display much more cooperativity among them (G.P. & A.A.K., unpublished results). One explanation of the differences in the functional epitopes for hPL and hGH is that their site1 interactions with hPRLR ECD1 are controlled by a higher level of cooperativity than

is found in the hGH:hGHR ECD1 interaction. A second point is that the binding sites on hGH to the hGHR ECDs have been shown to be allosterically coupled, one or two mutations in one site can change the structure and energetics of the binding interface of the other site over 20 Å away.[28,35] Therefore, even though the residue set comprising the structural epitopes of hPL and hGH differ at only a few positions, it is possible that other distal changes in the hormones near conformationally sensitive sites could induce small, but significant changes that manifest themselves by producing measurable alterations in the binding contributions of specific groups.

Materials and Methods

Sample preparation

Human placental lactogen and variants were expressed and purified as described.[6] The ECD (residues 1–211) of the hPRLR receptor was expressed at 20 °C and purified as described.[5] The free unpaired cysteine residue (C184) was mutated to alanine and serves as the wild-type receptor protein. The C184A-hPRLR does not affect binding affinity to the hormones.[5] The ECD of the hGHR (residues 29–238) containing a S237C mutation was grown and purified as described.[22,36] All mutations were made using Kunkel mutagenesis,[37] and confirmed by DNA sequencing. All protein purity and molecular masses were determined by analytical HPLC and mass spectrometry, respectively.

Selenomethionine (SeMet)-labeled hPL was grown using a modified AP5 minimal medium[38] substituting the Casamino acids with 19 amino acids and 50 mg l^{-1} of (L)-selenomethionine grown using the *met*$^-$ auxotroph B834 *Escherichia coli* cells (Novagen). SeMet-hPL was purified in exactly the same manner as the native hPL. Mass spectrometry showed incorporation of five or six SeMet sites (a total of six Met) into the hPL protein sequence.

Crystallization

Protein crystallization was performed using the sitting-drop, vapor-diffusion method at 19 °C. Native hPL crystals were produced from 2 μl of 6 mg ml^{-1} hPL (in 10 mM Tris–HCl (pH 7.5), 150 mM NaCl), 1 μl of 0.1 M sodium phosphate (pH 6.5), 2 μl from the reservoir solution (1 ml) containing 15% (v/v) PEG 3350. Cryoprotection for the native hPL crystal was achieved by increasing the concentration of glycerol to 20% (v/v) in the mother liquor. Native hPL crystals were flash-frozen into liquid propane.

A SeMet hPL crystal was produced from a sitting drop containing 1 μl of 3 mg ml^{-1} SeMet hPL (in 10 mM Tris–HCl (pH 7.5), 150 mM NaCl), 1 μl of 10 mM Tris–HCl (pH 7.5), 150 mM NaCl, 1 μl of a 1:10 (v/v) diluted native hPL seed crystal, and 1 μl of the reservoir solution (1 ml) of 19% (v/v) PEG 3350. A cut SeMet hPL crystal was flash-frozen into liquid nitrogen after increasing the concentration of glycerol to 20% glycerol in the mother liquor.

Data collection and structure determination

Native hPL and SeMet-hPL (three-wavelength MAD data set) data were collected at BioCARS 14BM-D and the Structural Biology Center 19ID beam lines at the Advanced Photon Source, respectively. All data were processed and scaled using the HKL2000 suite.[39] Monoclinic crystals for both the native and SeMet hPL belong to space group *C*2 with one molecule in the asymmetric unit. The positions of the selenium atoms (five sites found) for the SeMet hPL crystal were determined using SOLVE.[40] Density modification and initial chain tracing was carried out using RESOLVE to 2.7 Å.[40]

Refinement

Cross validation[41] of the wt-hPL structure was carried using a random 10% of the reflections for R_{free} determination before the start of refinement. Starting from the 2.7 Å MAD electron density map, multiple rounds of model-building were done using the program O,[42] and refinement using the native hPL data set from 15–2.0 Å. Phase extension from 2.7 Å to 2.0 Å, torsional angle dynamics simulated annealing, conjugate gradient energy minimization, and *B*-factor refinement were carried out using CNS.[43] Final refinement was performed using Refmac5[44] in the CCP4 suite.[45]

The final wt-hPL model consists of 161 out of 191 residues consisting of: 2–45, 51–60, 71–129, 137–148, and 154–189. Lys140 was modeled as alanine. The Ramachandran statistics for the final model, as determined by PROCHECK,[46] place 93.0% (132 residues) in the most favored regions, 5.6% (eight residues) in the additionally allowed regions, and 1.4% (two residues) in the generously allowed regions. The crystallographic and final refinement parameters are summarized in Table 1.

Surface plasmon resonance

Experiments were performed using a Biacore 2000 SPR instrument at 25 °C. Binding kinetics to the hGHR were determined by thiol coupling S237C-hGHR ECD to a C1 sensor chip as described.[22] The hPRLR ECD was coupled to a CM5 sensor chip using disulfide bond using an engineered C-terminal T207C mutation. Expressed T207C-hPRLR ECD contained a glutathione modification when expressed into the periplasm of *E. coli*. The glutathione modification was removed by incubating T207C-hPRLR with 1.5 mM DTT for 30 min at 4 °C. After reduction, the receptor was desalted into 10 mM sodium phosphate buffer (pH 7.4) using a PD-10 column (Amersham Biosciences), concentrated to ~300 μl and stored at 4 °C.

Initially, significant non-specific binding was observed over the underivatized flow-cell when either hPL or hGH was injected in the presence of Zn^{2+} buffer. This problem was determined to be due to effects of the required Zn^{2+} buffer and was eliminated by blocking the unreactive sites after derivatization of the flow-cells with or without T207C-hPRLR by sequential injections of reduced glutathione (to block unreactive SH groups) and ethanolamine (to block unreactive NH groups). This coupling strategy may be of general utility for measuring biological interactions by SPR involving metal coordination.

The CM5 sensor chip preparation was carried out in HBS-EP buffer (10 mM Hepes (pH 7.4), 150 mM NaCl, 3 mM EDTA, 0.005% (v/v) TWEEN-20). The sensor chip

was prepared by washing with HBS-EP buffer at a flow-rate of 5 μl min^{-1}, followed by activation of each flow-cell with a 10 μl injection of NHS/EDC (*N*-hydroxysuccinimide (75 mg ml^{-1})/*N*-ethy-*N*′-(3-dimethylaminopropyl)carbodiimide (11.5 mg ml^{-1})), then injection of 20 μl of 18 mg ml^{-1} PDEA (2-(2-pyridinyldithio)ethaneamine hydrochloride in 50 mM $NaHCO_3$ (pH 8.5) and finally, injection of 30 μl of 50–100 μg ml^{-1}reduced T207C-hPRLR (typically 30 μl of hPRLR plus 100 μl of 10 mM sodium acetate, pH 4.5). Flow cells 2–4 were coupled with T207C-hPRLR, while flow-cell 1 was activated but no T207C-hPRLR was injected, serving as a reference cell). The flow-cells were sequentially blocked with a injection of 35 μl of 50 mM reduced glutathione in 20 mM sodium acetate (pH 4.5) with 1 M NaCl and injection of 35 μl of 1 M ethanolamine (pH 8.5).

SPR experiments were performed at a flow-rate of 50 μl min^{-1} in HBS-EP buffer or TBS-P Zn^{2+} buffer (10 mM Tris–HCl (pH 7.5), 150 mM NaCl, 0.05% TWEEN-20, 50 μM $ZnCl_2$ (Puratronic grade, Alfa Aesar)). Twofold serial dilutions of five concentrations typically starting at 40 nM or 200 nM were injected for each hormone variants. Each injection of 250 μl of protein/buffer was followed by a 600 s dissociation period. The surface was regenerated for subsequent runs with injection of 10 μl of 4.5 M $MgCl_2$. Approximately, 100–200 injections were made on a sensor chip surface. The six sensorgrams for each binding experiment were globally fit to a simple 1:1 Langmuir binding model in either the BIAevaluation 3.1 or the ClampXP[47] software packages. Each protein variant was measured in triplicate, and the average rate constants are reported. The rate constants showed less than 5% difference in replicated measurements.

Protein Data Bank accession code

The hPL coordinates have been deposited with the Protein Data Bank under accession code 1z7c.

Acknowledgements

We thank Drs B. Gopal, Julie Dohm, and Apostolos Gittis for advice and help with the crystallography. We thank the staffs of BioCARS and the Structural Biology Center for help with data collection. Use of the Advanced Photon Source was supported by the US Department of Energy, Basic Energy Sciences, Office of Science, under contract no. W-31-109-Eng-38. Use of the BioCARS Sector 14 was supported by the US National Institutes of Health (NIH), National Center for Research Resources, under grant RR07707. S.T.R.W. was a Burroughs Wellcome Fund fellow of the Life Sciences Research Foundation. This work was supported by the NIH grant DK-61602 to A.A.K.

References

1. Goffin, V. & Kelly, P. A. (1997). The prolactin/growth hormone receptor family: structure/function relationships. *J. Mammary Gland Biol. Neoplasia*, **2**, 7–17.
2. Genuth, S. M. (1988). In *The Endocrine System. Physiology* (Berne, R. M. & Levy, M. N., eds) *The Endocrine System. Physiology* 2nd edit., C.V. Mosby Company, St. Louis, MI.
3. Fuh, G., Colosi, P., Wood, W. I. & Wells, J. A. (1992). Rational design of potent antagonists to the human growth hormone receptor. *Science*, **268**, 5376–5381.
4. Fuh, G. & Wells, J. A. (1995). Prolactin receptor antagonists that inhibit the growth of breast cancer cell lines. *J. Biol. Chem.* **270**, 13133–13137.
5. Cunningham, B. C., Bass, S., Fuh, G. & Wells, J. A. (1990). Zinc mediation of the binding of humane growth hormone to the human prolactin receptor. *Science*, **250**, 1709–1712.
6. Lowman, H. B., Cunningham, B. C. & Wells, J. A. (1991). Mutational analysis and protein engineering of receptor-binding determinants in human placental lactogen. *J. Biol. Chem.* **266**, 10982–10988.
7. Goffin, V., Binart, N., Touraine, P. & Kelly, P. A. (2002). Prolactin: the new biology of an old hormone. *Annu. Rev. Physiol.* **64**, 47–67.
8. Wells, J. A. (1996). Binding in the growth hormone receptor complex. *Proc. Natl Acad. Sci. USA*, **93**, 1–6.
9. Kossiakoff, A. A. & de Vos, A. M. (1998). Structural basis for cytokine hormone-receptor recognition and receptor activation. *Advan. Protein Chem.* **52**, 67–108.
10. Kossiakoff, A. A. (2004). The structural basis for biological signaling, regulation, and specificity in the growth hormone-prolactin system of hormones and receptors. *Advan. Protein Chem.* **68**, 147–169.
11. Herman, A., Helman, D., Livnah, O. & Gertler, A. (1999). Ruminant placental lactogens act as antagonists to homologous growth hormone receptors and as agonists to human or rabbit growth hormone receptors. *J. Biol. Chem.* **274**, 7631–7639.
12. Herman, A., Bignon, C., Daniel, N., Gosclaude, J., Gertler, A. & Dijane, J. (2000). Functional heterodimerization of prolactin and growth hormone receptors by ovine placental lactogen. *J. Biol. Chem.* **275**, 6295–6301.
13. Elkins, P. A., Christinger, H. W., Sandowski, Y., Sakal, E., Gertler, A., de Vos, A. M. & Kossiakoff, A. A. (2000). Ternary complex between placental lactogen and the extracellular domain of the prolactin receptor. *Nature Struct. Biol.* **7**, 808–815.
14. Somers, W., Ultsch, M., de Vos, A. M. & Kossiakoff, A. A. (1994). The X-ray structure of a growth hormone-prolactin receptor complex. *Nature*, **372**, 478–481.
15. Hendrickson, W. A. (1991). Determination of macromolecular structures from anomalous diffraction of synchrotron radiation. *Science*, **254**, 51–58.
16. de Vos, A. M., Ultsch, M. & Kossiakoff, A. A. (1992). Human growth hormone and extracellular domain of its receptor: crystal structure of the complex. *Science*, **255**, 306–312.
17. Teilum, K., Hoch, J. C., Goffin, V., Kinet, S., Martial, J. A. & Kragelund, B. B. (2005). Solution structure of human prolactin. *J. Mol. Biol.* **351**, 810–823.
18. Abdel-Meguid, S. S., Shieh, H. S., Smith, W. W., Dayringer, H. E., Violand, B. N. & Bentle, L. A. (1987). Three-dimensional structure of a genetically engineered variant of porcine growth hormone. *Proc. Natl Acad. Sci. USA*, **84**, 6434–6437.
19. Clackson, T., Ultsch, M. H., Wells, J. A. & de Vos, A. M. (1998). Structural and functional analysis of the 1:1 growth hormone:receptor complex reveals the molecular basis for receptor affinity. *J. Mol. Biol.* **277**, 1111–1128.
20. Kasimova, M. R., Kristensen, S. M., Howe, P. W., Christensen, T., Matthiesen, F., Petersen, J. *et al*. (2002).

NMR studies of the backbone flexibility and structure of human growth hormone: a comparison of high and low pH conformations. *J. Mol. Biol.* **318**, 679–695.
21. Kossiakoff, A. A., Somers, W., Ultsch, M., Andow, K., Muller, Y. A. & de Vos, A. M. (1994). Comparison of the intermediate complexes of human growth hormone bound to the human growth hormone and prolactin receptors. *Protein Sci.* **3**, 1697–1705.
22. Walsh, S. T., Jevitts, L. M., Sylvester, J. E. & Kossiakoff, A. A. (2003). Site2 binding energetics of the regulatory step of growth hormone-induced receptor homodimerization. *Protein Sci.* **12**, 1960–1970.
23. Cunningham, B. C. & Wells, J. A. (1991). Rational design of receptor-specific variants of human growth hormone. *Proc. Natl Acad. Sci. USA*, **88**, 3407–3411.
24. Sivaprasad, U., Canfield, J. M. & Brooks, C. L. (2004). Mechanism for ordered receptor binding by human prolactin. *Biochemistry*, **43**, 13755–13765.
25. Bernat, B., Sun, M., Dwyer, M., Feldkamp, M. & Kossiakoff, A. A. (2004). Dissecting the binding energy epitope of a high-affinity variant of human growth hormone: cooperative and additive effects from combining mutations from independently selected phage display mutagenesis libraries. *Biochemistry*, **43**, 6076–6084.
26. Cunningham, B. C. & Wells, J. A. (1993). Comparison of a structural and a functional epitope. *J. Mol. Biol.* **234**, 554–563.
27. Bernat, B., Pal, G., Sun, M. & Kossiakoff, A. A. (2003). Determination of the energetics governing the regulatory step in growth hormone-induced receptor homodimerization. *Proc. Natl Acad. Sci. USA*, **100**, 952–957.
28. Walsh, S. T., Sylvester, J. E. & Kossiakoff, A. A. (2004). The high- and low-affinity receptor binding sites of growth hormone are allosterically coupled. *Proc. Natl Acad. Sci. USA*, **101**, 17078–17083.
29. Kouadio, J. L., Horn, J. R., Pal, G. & Kossiakoff, A. A. (2005). Shotgun alanine scanning shows that growth hormone can bind productively to its receptor through a drastically minimized interface. *J. Biol. Chem.* **280**, 25524–25532.
30. Liparoto, S. F. & Ciardelli, T. L. (1999). Biosensor analysis of the interleukin-2 receptor complex. *J. Mol. Recogn.* **12**, 316–321.
31. Shen, B. J., Hage, T. & Sebald, W. (1996). Global and local determinants for the kinetics of interleukin-4/interleukin-4 receptor alpha chain interaction. A biosensor study employing recombinant interleukin-4-binding protein. *Eur. J. Biochem.* **240**, 252–261.
32. Wang, Y., Shen, B. J. & Sebald, W. (1997). A mixed-charge pair in human interleukin 4 dominates high-affinity interaction with the receptor alpha chain. *Proc. Natl Acad. Sci. USA*, **94**, 1657–1662.
33. Hensley, P., Doyle, M. L., Myszka, D. G., Woody, R. W., Brigham-Burke, M. R., Erickson-Miller, C. L. *et al.* (2000). Evaluating energetics of erythropoietin ligand binding to homodimerized receptor extracellular domains. *Methods Enzymol.* **323**, 177–207.
34. Nice, E., Layton, J., Fabri, L., Hellman, U., Engstrom, A., Persson, B. & Burgess, A. W. (1993). Mapping of the antibody- and receptor-binding domains of granulocyte colony-stimulating factor using an optical biosensor. Comparison with enzyme-linked immunosorbent assay competition studies. *J. Chromatog.* **646**, 159–168.
35. Schiffer, C., Ultsch, M., Walsh, S., Somers, W., de Vos, A. M. & Kossiakoff, A. (2002). Structure of a phage display-derived variant of human growth hormone complexed to two copies of the extracellular domain of its receptor: evidence for strong structural coupling between receptor binding sites. *J. Mol. Biol.* **316**, 277–289.
36. Fuh, G., Mulkerrin, M. G., Bass, S., McFarland, N., Brochier, M., Bourell, J. H. *et al.* (1990). The human growth hormone receptor. *J. Biol. Chem.* **265**, 3111–3115.
37. Kunkel, T. A., Roberts, J. D. & Zakour, R. A. (1987). Rapid and efficient site-specific mutagenesis without phenotypic selection. *Methods Enzymol.* **154**, 367–382.
38. Chang, C. N., Rey, M., Bochner, B., Heyneker, H. & Gray, G. (1987). High-level secretion of human growth hormone by *Escherichia coli*. *Gene*, **55**, 189–196.
39. Otiwinowski, Z. & Minor, W. (1997). Processing of X-ray diffraction data collected in oscillation mode. In *Methods in Enzymology* (Carter, C. W. J. & Sweet, R. M., eds), vol. 276, pp. 307–326, Academic Press, New York.
40. Terwilliger, T. C. (2003). SOLVE and RESOLVE: automated structure solution and density modification. *Methods Enzymol.* **374**, 22–37.
41. Brunger, A. T. (1993). Assessment of phase accuracy by cross validation: the free R value. Methods and applications. *Acta Crystallog. sect. D*, **49**, 24–36.
42. Jones, T. A., Zou, J. Y., Cowan, S. W. & Kjeldgaard, M. (1991). Improved methods for building protein models in electron density maps and the location of errors in these models. *Acta Crystallog. sect. A*, **47**, 110–119.
43. Brunger, A. T., Adams, P. D., Clore, G. M., DeLano, W. L., Gros, P., Grosse-Kunstleve, R. W. *et al.* (1998). Crystallography NMR system: a new software suite for macromolecular structure determination. *Acta Crystallog. sect. D*, **54**, 905–921.
44. Murshudov, G. N., Vagin, A. A. & Dodson, E. J. (1997). Refinement of macromolecular structures by the maximum-likelihood method. *Acta Crystallog. sect. D*, **53**, 240–255.
45. Collaborative Computing Project Number 4. (1994). The CCP4 suite: programs for protein crystallography. *Acta Crystallog. sect. D*, **50**, 760–763.
46. Laskowski, R., MacArthur, M., Moss, D. & Thornton, J. (1993). PROCHECK: a program to check the stereochemical quality of protein structures. *J. Appl. Crystallog.* **26**, 283–291.
47. Myszka, D. G. & Morton, T. A. (1998). Clamp: a biosensor kinetic data analysis program. *Trends Biochem. Sci.* **23**, 149–150.
48. Thompson, J. D., Higgins, D. G. & Gibson, T. J. (1994). CLUSTAL W: improving the sensitivity of progressive multiple sequence alignment through sequence weighting, position-specific gap penalties and weight matrix choice. *Nucl. Acids Res.* **22**, 4673–4680.

Edited by I. Wilson

(Received 5 January 2006; received in revised form 10 February 2006; accepted 14 February 2006)
Available online 2 March 2006